

4×4 STRICTLY NON-BLOCKING OPTICAL SWITCH FABRIC BASED ON CASCADED MULTIMODE INTERFEROMETERS

Zuxiang Li, Linjie Zhou*, Liangjun Lu, and Jianping Chen

State Key Laboratory of Advanced Optical Communication Systems and Networks
Department of Electronic Engineering, Shanghai Jiao Tong University, Shanghai 200240, China
*ljzhou@sjtu.edu.cn

ABSTRACT

We experimentally demonstrate a 4×4 strictly non-blocking silicon thermo-optic (TO) switch fabric consisting of three stages of tunable generalized Mach-Zehnder interferometers. Measurements show that the worst crosstalk of all switching states is -7.16 dB. The average TO switching power consumption is 104.84 mW.

Keywords: Silicon photonics, Optical switches, Mach-Zehnder interferometers, Multimode interference (MMI)

1. INTRODUCTION

Continuous increase in the network traffic for both optical communications and photonic networks-on-chip requires vast demand of integrated optical switches [1-3]. An N×N optical switch is usually constructed by 1×2 or 2×2 switch elements, such as Mach-Zehnder interferometers (MZIs) and microring resonators (MRRs). In comparison with MRRs, MZI-based switches have a broader optical bandwidth and better tolerance to environmental temperature variations [4]. Multimode interference (MMI) couplers are widely used as splitters and combiners in MZIs since they possess the desirable attributes of small size, low excess loss, well-defined splitting, dimensional tolerance, and ease of fabrication. By connecting multi-port MMIs using an array of phase shifters, the so-called generalized Mach-Zehnder interferometer (GMZI) can be formed [5]. The GMZI can function as a 1×N or N×N switch. Silicon provides an attractive material platform for developing photonic switches by allowing for monolithic integration of optics and electronic control circuits on a same chip [6]. A variety of thermo-optic (TO) silicon waveguide switches have been demonstrated in the past due to the relatively high thermal conductivity and TO coefficient of silicon ($\partial n/\partial T = 1.86 \times 10^{-4} \text{ K}^{-1}$ at 300K).

In this paper, we report the experimental realization of a silicon 4×4 strictly non-blocking optical switch based on cascaded GMZIs. The footprint of this chip is

4.64×1.00 mm². The worst crosstalk for all switching states is -7.16 dB. Section II gives the details of the switch architecture. The experiment and characterization of the device are presented in Section III.

2. DEVICE DESIGN AND FABRICATION

Figure 1(a) shows the switch architecture consisting of three stages of GMZIs. The cascaded architecture requires the minimum number of switching elements to obtain the full switch states. For the GMZI structure, when one connection is established, the other three connections for a particular switch state is uniquely defined. Therefore, a single N×N GMZI switch only has N different switching states [4, 5, 7]. As a consequence, the 4×4 GMZI (GM4) in Fig. 1(a) is incomplete to form a non-blocking switch with 4!=24 switching states. To achieve the full connections, we cascade a 3×3 GMZI (GM3) and a 2×2 GMZI (GM2) to the GM4. Therefore, this cascaded structure can generate 4×3×2=24 permutations to form a strictly non-blocking switch.

To change the phase of GMZI arms for switching operation, TO phase shifters based on silicon resistive microheaters are utilized [8]. Figure 1(b) shows the cross-sectional schematic of the silicon resistive microheaters. Figure 1(c) shows all the possible switching states for the 4×4, 3×3, and 2×2 GMZIs.

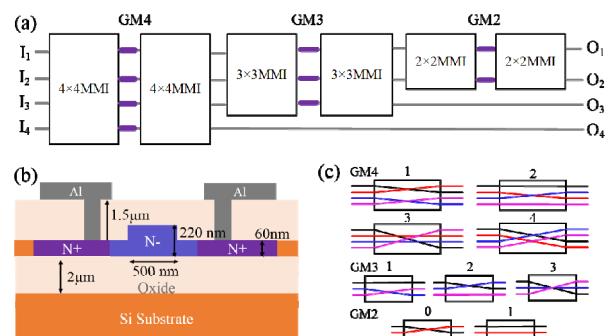


Fig. 1 (a) 4×4 cascaded GMZI switch structure. (b) Cross-sectional schematic of TO phase shifter. (c) Switching states of single GMZIs.

The switch was fabricated on a silicon-on-insulator (SOI) wafer. The silicon waveguide has a dimension of $0.5 \mu\text{m}$ (width) \times $0.22 \mu\text{m}$ (height) with a slab thickness is $0.06 \mu\text{m}$. Ion implantation of phosphorus was used to form N^- doped region with a doping concentration of $8 \times 10^{16} \text{cm}^{-3}$ to reduce resistance and simultaneously maintain low propagation loss for the waveguides. The heavily N^+ doped regions have a doping concentration of 10^{20}cm^{-3} for good ohmic contact. Rapid thermal annealing (RTA) at 1030°C for 5 seconds was used after ion implantation. Then a $1.5 \mu\text{m}$ thick oxide was deposited on waveguides using the plasma-enhanced chemical vapor deposition (PECVD) as upper cladding. Finally, contact via holes were etched and aluminum connection was formed by sputtering and plasma dry etch. The whole fabrication process was CMOS compatible.

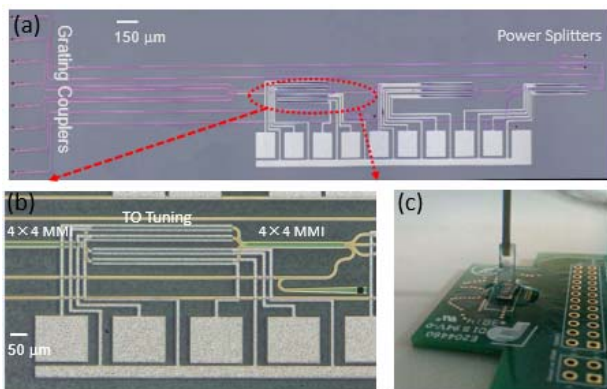


Fig. 2 (a) Optical microscope image of the fabricated 4×4 switch. (b) Zoom-in view of the GMZI switching element. (c) Packaged switch chip.

Figure 2(a) shows the optical microscope image of the fabricated 4×4 switch. The size of the device is $4.64 \times 1.00 \text{mm}^2$, including all the electrical pads and fiber array coupling region. Grating couplers with a $0.63 \mu\text{m}$ period and $0.07 \mu\text{m}$ shallow etch depth are used for input and output coupling. In our design we purposely added a directional coupler in each output waveguide so that light can be coupled out of the chip from both the left side (fiber array coupling) and the right side (individual fiber coupling) for easy testing. The directional coupler is designed to have a gap of 200nm and a coupling length of $13 \mu\text{m}$. The splitting loss at the fiber array end is about 4.8dB based on the finite-difference time-domain (FDTD) simulation. The metal pads were wire-bonded to a print circuit board (PCB). Finally, an 8-channel fiber array was aligned and attached to the chip by using UV light curable adhesive, whose refractive index is close to the refractive index of SiO_2 . The additional loss of the fiber array after package is about 2dB . Figure 2(c) shows the photo of the packaged switch chip.

3. EXPERIMENT AND RESULTS

Light was coupled to one input port, and a routing path from the input port to a specific output port was determined by applying proper voltages on TO phase shifters. We monitored this routing path by measuring the transmitted optical power through an optical power meter. Apart from the main path, the optical power is also partially coupled to the other three output ports, leading to crosstalk. For each switching state, we measured the crosstalk of the four optical paths. The TO power consumption of each switching state was measured with an average value of 104.84mW . The power consumption can be further reduced by using isolation grooves to minimize thermal leakage [9].

The crosstalk induced by the input port m ($m \neq i$) to the routing path $I_i \rightarrow O_j$ ($i, j = 1, 2, 3, \text{ and } 4$) is defined as the ratio of leaked output power $P_{\text{out}(m \rightarrow j)}$ to the output power $P_{\text{out}(i \rightarrow j)}$ [4]. The device crosstalk is then defined as the worst crosstalk of all routing paths. The crosstalk of our switch was measured to be -7.16dB at 1533nm operation wavelength, which is mainly caused by the power splitting imbalance of MMIs.

Figure 3 shows the measured transmission spectra for one switching state. In each plot, transverse electric (TE) polarized light was launched from four input ports and the spectra from one particular output port were recorded. The transmission loss consists of coupling loss, additional fiber array packaging loss, power splitting loss, and on-chip insertion loss. Because of the imbalanced arms between MMIs, the spectra exhibit periodic interference pattern. At 1533nm , we get input and output routing relationship as I_2-O_1 , I_4-O_2 , I_3-O_3 , and I_1-O_4 . The power consumption for this switching state is 107.64mW .

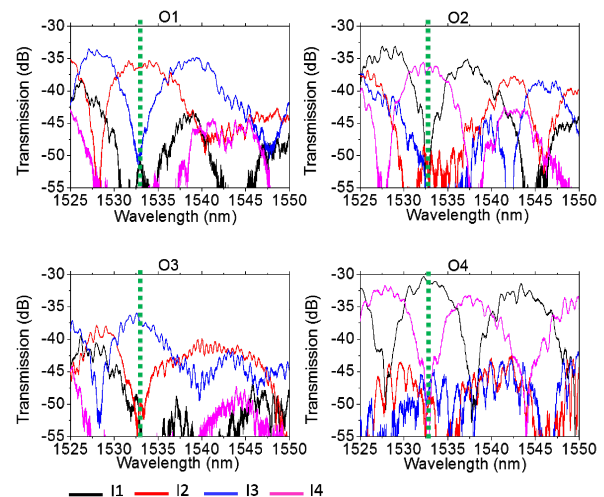


Fig. 3 Measured transmission spectra at the four output ports of the switch when it is configured as I_2-O_1 , I_4-O_2 , I_3-O_3 , and I_1-O_4 .

Figure 4 shows the spectra for another switching state with input and output ports mapped as I_3-O_1 , I_1-O_2 , I_2-O_3 , and I_4-O_4 . The power consumption for this state is 142.07mW .

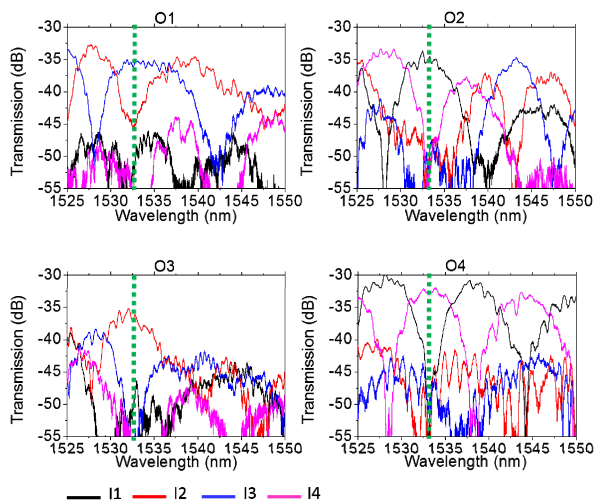


Fig. 4 Measured transmission spectra at the four output ports of the switch when it is configured I_3 - O_1 , I_1 - O_2 , I_2 - O_3 , and I_4 - O_4 .

From the spectra of the two switching states, one observes that transmission to O_4 has the lowest loss, which is expectable as light only goes through GM4. Transmissions to O_1 , O_2 and O_3 have a similar loss level, but all higher than transmission to O_4 , which suggests GM3 might have a higher insertion loss than GM4 and GM2. In our design, we used three-dimensional (3D) beam propagation method (BPM), which is not accurate enough for high index contrast silicon waveguides. The insertion loss of switch fabric would be reduced if the MMIs were optimized using 3D finite-difference time-domain (FDTD) method.

4. CONCLUSION

We have demonstrated a 4×4 strictly non-blocking silicon TO switch based on cascaded GMZIs. Experimental results show that the switch crosstalk is -7.16 dB and the average power consumption is 104.84 mW. The performance of the 4×4 optical switch can be further improved by optimizing the 4×4 and 3×3 and 2×2 MMIs with a lower loss and a higher power splitting uniformity.

5. ACKNOWLEDGEMENTS

This work was supported in part by the 973 program (2011CB301700), the 863 program (2013AA014402), the National Natural Science Foundation of China (NSFC) (61422508), Science and Technology Commission of Shanghai Municipality (STCSM) Project (14QA1402600). We also acknowledge IME Singapore for device fabrication.

6. REFERENCES

- [1] B. G. Lee, A. V. Rylyakov, W. M. J. Green, S. Assefa, C. W. Baks, R. Rimolo-Donadio, *et al.*, "Monolithic Silicon Integration of Scaled Photonic Switch Fabrics, CMOS Logic, and Device Driver Circuits," *Journal of Lightwave Technology*, vol. 32, pp. 743-751, 2014.
- [2] K. Suzuki, K. Tanizawa, T. Matsukawa, G. Cong, S. H. Kim, S. Suda, *et al.*, "Ultra-compact 8×8 Strictly-non-blocking Si-wire PILOSS Switch," *Opt Express*, vol. 22, pp. 3887-94, Feb 24 2014.
- [3] L. Zhou, L. Lu, Z. Li, and J. Chen, "Broadband 4×4 Non-blocking Optical Switch Fabric Based on Mach-Zehnder Interferometers," *13th International Conference on Optical Communications and Networks (ICOON)*, pp. 1-4, 2014.
- [4] L. Lu, L. Zhou, S. Li, Z. Li, X. Li, and J. Chen, " 4×4 Nonblocking Silicon Thermo-Optic Switches Based on Multimode Interferometers," *Journal of Lightwave Technology*, vol. 33, pp. 857-864, 2015.
- [5] L. W. Cahill, "The Modelling of Integrated Optical Power Splitters and Switches Based on Generalised Mach-Zehnder Devices," *Optical and Quantum Electronics*, vol. 36, pp. 165-173, 2004.
- [6] D. Patel, V. Veerasubramanian, S. Ghosh, W. Shi, A. Samani, Q. Zhong, *et al.*, "A 4×4 fully Non-blocking Switch on SOI Based on Interferometric Thermo-optic Phase Shifters," *2014 IEEE Optical Interconnects Conference*, pp. 104-105, 2014.
- [7] W. Wang, H. Zhou, J. Yang, M. Wang, and X. Jiang, "Highly Integrated 3×3 Silicon Thermo-optical Switch Using a Single Combined Phase Shifter for Optical Interconnects," *Opt Lett*, vol. 37, pp. 2307-9, Jun 15 2012.
- [8] L. Zhou, X. Zhang, L. Lu, and J. Cheng, "Tunable Vernier Microring Optical Filters With p-i-p Type Microheaters," *IEEE Photonics Journal*, vol. 5, pp. 6601211-6601211, 2013.
- [9] H. Zhou, J. Song, E. K. Chee, C. Li, H. Zhang, and G. Lo, "A Compact Thermo-optical Multimode-interference Silicon-based 1×4 Nano-photonic Switch," *Opt Express*, vol. 21, pp. 21403-13, Sep 9 2013.